Separating the contributions of zona pellucida and cytoplasm in the viscoelastic response of human oocytes.

Tong Shen[1] Eduard Benet[1] Shankar Lalitha Sridhar[1], Joel Abadie[2], Emmanuel Piat[2] and Franck J. Vernerey[1,*]

1. University of Colorado at Boulder, Department of Mechanical Engineering
2. FEMTO-ST Institute, UMR CNRS 6174, UFC - ENSMM - UTBM, Besancon, France
(Dated: November 22, 2018)

The successful characterization of the mechanical properties of human oocytes and young embryos is of crucial relevance to reduce the risk of pregnancy arrest in in-vitro fertilization processes. Unfortunately, current study has been hindered by the lack of accuracy in describing the mechanical contributions of each structure (zona pellucida, cytoplasm) due to its high heterogeneity. In this work, we present a novel approach to model the oocyte response taking into account the effect of both zona and cytoplasm, as well as different loading conditions. The model is then applied to develop an experimental protocol capable of accurately separating the viscoelastic contribution of zona and cytoplasm by simply varying the loading condition. This new protocol has the potential to open the door to improving our understanding the mechanical properties of oocytes at different stages, and provide a quantitative predictive ability to the evaluation of oocyte quality.

Keywords: Oocyte, compression/indentation tests, modified Hertz contact, experimental protocol

I. INTRODUCTION

The success of assisted reproductive technologies is often linked to the quality of the chosen oocytes [1, 2]. Significant research effort has therefore been dedicated to predicting the quality of an oocyte before [3] and after fertilization [4] with the prospect of reducing the risk of pregnancy arrest and increasing the implantation success. Generally, the quality of an oocyte has been linked to its appearance, wherein a rounded cell with clear, moderately granular cytoplasm, a small perivitelline space, and a clear to colorless zona pellucida is usually preferred (see Fig. 2) [5, 6]. Oocyte selection based on morphology has perdured until now where figures of merit such as the thickness of the zona pellucida [7], the granularity of the cytoplasm [8] and the general shape of an oocyte [9] were brought up as major indications of fertility. The use of such subjective criteria is, however, becoming controversial as morphological traits, often interpreted as indications of developmental malfunctions [10], may only be artifacts of natural variability [11]. A number of recent studies have therefore attempted to identify alternative, and perhaps more objective measures to not only select the best oocytes but also their appropriate maturation stage to yield the highest chance of fertilization. In the general context of cell biology, mechanical properties are known to be excellent indicators of a cell's physical state regarding disease [12–14], differentiation [15], or cancer detection [16, 17]. In the case of oocytes, Palermo et al. [17] were the first to show that the rupture of the oolemma during intracytoplasmic injection is an accurate indication of a cell's fate. Since then, a number of experimental and theoretical approaches have been developed to measure and classify the oocytes based on mechanical properties. Experimental methods were actually developed as early as 1969, when Hiramoto and Nemoto [18, 19] used parallel plate compression and micropipette aspiration to measure the surface stiffness of a variety of oocytes. It was, however, not until recent years that researchers used micro-indentation and micropipette aspiration to characterize temporal changes in oocyte properties during maturation [20–26]. Among these studies, Liu et al. [26] reported that aged oocytes, with presumably low fertilization potential, were significantly softer and more viscous compared to younger ones. This study was the first to report a clear relationship between mechanical properties and oocyte quality. The key role of mechanics was further confirmed by the work of Yanez et al. [23, 27] who unequivocally correlated the developmental potential of zygotes to their stiffness. While cell malfunction is attributed to either incomplete zona hardening [28], or insufficient softening during maturation, its precise origin from a molecular perspective, is still obscure.

Mechanics, thus, appears to be a promising indicator, but it usually encompasses a variety of behavior including its elastic response, that may and may not be linear; a time-dependent, or viscoelastic response; or even failure properties, defined by the rupture of its components. As these mechanisms usually occur simultaneously, the interpretation of mechanical tests typically requires the assistance of mathematical models. One of the most common approaches consists of using a so-called Zener model, which approximates the oocyte as a integrated system of elastic and viscous elements. By fitting the properties of these elements to the measured response, it is, therefore, possible to obtain a set of measurable quantities (such as stiffness and viscosity) that can be correlated to the oocyte's chances of fertilization. Despite its ease of use, this approach suffers from a lack of connection between loading conditions, the multi-layered structure of the cell, and its mechanical response. In other words, it is incapable of distinguishing the cause from the effect

---

* Correspondence: Franck.Vernerey@colorado.edu
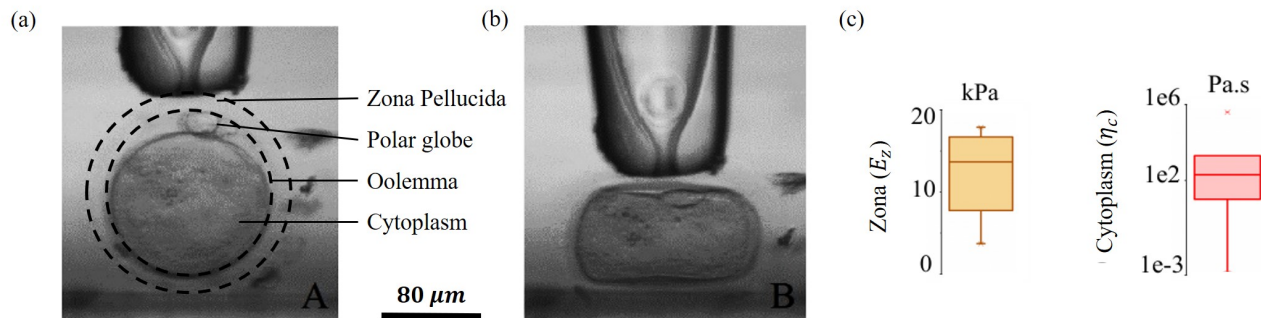
FIG. 1. *(a) The profile of an oocyte at its undeformed state. (b) An experimental snapshot about the oocyte being indented. (c) The reported literature values for the oocyte properties including the viscosity of the cytoplasm η_c [19, 29–44] and the elastic modulus of the zona E_z [24, 45–48] in mamalian cells. The values include measurements from murine, porcine, and human cells.*

that is important for identifying the origin of an oocyte's malfunction. To overcome these limitations, more accurate mechanical models, accounting for the oocyte geometry and deformation, have been recently proposed. For instance, Sun et al. [45] derived an elastic membrane model that can be used to determine the properties of the zona pellucida, while Liu et al. [26] introduced a three-dimensional finite element approach to treat the cell as a homogeneous hyperelastic body. These models have shown promise in better understanding the origin of the oocyte's response, but still remain too simplistic to capture its time-dependent response and the distinct roles of the cytoplasm and zona pellucida, both of which have been identified as key indicators of an oocyte's developmental fate [9]. Based on these observations, Yanez et al. [27] identified two clear needs in terms of theoretical developments. On the one hand, future models must establish a correlation between the oocyte's viscoelastic response and its molecular structures. On the other hand, such models need to clearly distinguish the effects of the zona pellucida, the cytoplasm, and their interactions, as they are likely to play distinct roles in the fertilization potential of the cell.

In this paper, we tackle this challenge by proposing an alternative solution to the standard Zener model in order to accurately capture the viscoelastic response of an oocyte. Specifically, the distinct contributions of the zona and cytoplasm and the role of boundary conditions under indentation are clearly identified. For this, we view an oocyte as a heterogeneous structure, made up by the cytoplasm and the zona pellucida, each represented by their own viscoelastic properties. Using transient network theory [49, 50], these properties are directly related to the molecular mechanics of the underlying biopolymer, and the oocyte deformation under arbitrary loads can be simulated using finite-element analysis. The model is calibrated with a set of experimental data on human oocytes representing their elastic and stress relaxation responses under compression [20]. This numerical approach is then used to construct a simplified semi-

analytical model based on modified Hertz contact theory for viscoelasticity [51]. To illustrate the potential of this new method, we then propose an experimental protocol that, in conjunction with the modified Hertz model, is capable of separating the roles of zona and cytoplasm on the overall viscoelasticity of an oocyte.

II. PHYSICAL MODEL OF A HUMAN OOCYTE

When observed under a microscope, an oocyte reveals four distinct regions (Fig. 1a): the cytoplasm, the oolemma, the zona pellucida, and the polar globe. The cytoplasm makes the interior compartment of the cell and consists of a biorheological fluid encapsulated within a thin lipid bilayer known as the oolemma. This region is further surrounded by a $10 \sim 15 \ \mu m$ thick zona pellucida whose mechanical properties significantly differ from those of the cytoplasm. The function of this layer has been linked to oocyte protection, fertilization, hatching, and transport [24] to name a few. As discussed above, the quality of an oocyte is likely related to the mechanical properties (or their change) of each of these components.

Although the oocyte mechanics can be characterized in a multitude of ways, depending on the property of interest, the testing of oocytes for in-vitro fertilization is typically constrained to simple, fast, and non-invasive methods. Among those, micro-pipette aspiration [23] and indentation tests [25, 26] have been the most popular in the literature. However, these tests give access to macroscopic force (or pressure)- displacement relationships that need to be translated into physical measurements (such as an equivalent elastic modulus and viscosity). This task is not trivial since measurements are characteristic of the entire oocyte and do not help in distinguishing between the roles of its different components. A solution to this problem can be found by introducing models that are physically more accurate while containing a small number of physically-relevant parameters. This section starts by reporting the mechanical
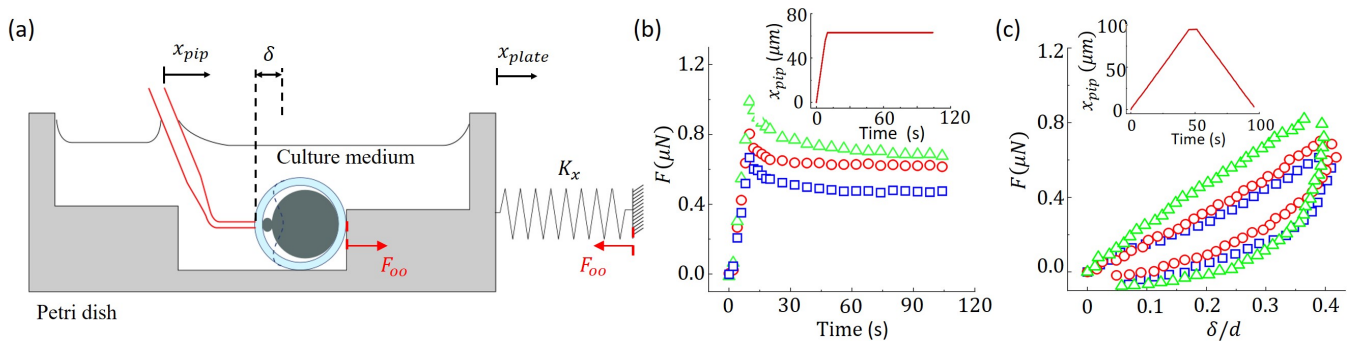
FIG. 2. *(a) The schematic of the flotation platform used as a nanosensor [20]. (b) Stress relaxation tests performed on three different oocytes, where each of them was indented at a speed $v = 7\mu m$ until a total displacement of $\delta = 60\mu m/s$ was achieved, and then they were allowed to relax at a constant deformation. (c) Loading-unloading results on the same three oocytes with a loading/unloading speed of $v = 2.5\mu m/s$ and intermediate pause of 4s. Different symbols (gree triangle, red circle and blue square) were used to represent experimental data obtained from three different oocytes*

response of human oocytes under indentation (Fig. 1b). These results are then used to construct a high-fidelity computational model of the oocyte accounting for the distinct mechanical properties of zona and cytoplasm.

A. Experimental characterization of oocytes

One of the challenges in studying the oocyte mechanical response lies in the fact that reported properties among research groups show a great disparity (Fig. 1c), which cannot be explained by the normal variations in biological systems. These may particularly arise from two different sources, including (a) the challenge of measuring accurate forces in such small and soft systems (at the scale of nano-Newtons) and (b) the lack of a standarized testing protocol that can uniformly measure the same compartment properties. To address the first issue, we have recently introduced a measuring platform with the capability of determining a force applied to oocyte at the scale of nano-Newtons [20]. More precisely, the testing device consists of a petri dish (in which the oocyte is placed) connected to a magnetic spring with known stiffness K_x (Fig.2a). Oocyte indentation can then be performed by controlling the displacement x_{pip} of a micropipette that plays the role of the indenter. The indentation depth δ of the oocyte is measured as the difference in displacement between the petri dish x_{plat} and the pipette as $\delta = x_{pip} - x_{plat}$. The resulting force may then be back-calculated using the knowledge of the petri dish displacement x_{plat} via Hooke's law $F_{oo} = K_x \cdot x_{plat}$.

Using this magnetic flotation platform, the characteristic response of oocytes of average diameter $d = 150 \pm 8 \ \mu m$ in the MII stage is assessed by compressing them by a large indenter with a semi-circular tip of radius $45 \ \mu m$. To fully capture the time-dependent response of the oocytes, wo chose to perform two standard types of experimental loadings to extract viscoelastic properties: a standard stress-relaxation test and a loading-unloading

cycle. During the stress relaxation tests, oocytes are compressed at a faster rate of $\dot{x}_{pip} = 7 \ \mu m/s$, so that the time-dependent response is significant, until a total pipette displacement of $x_{pip} = 60 \ \mu m$, or equivalently in strain $\delta/d = 0.4$, is completed. The oocyte is then allowed to relax by holding the pipette displacement for a total of 100 seconds. During the loading-unloading cycle, the indenter is first moved downwards with a constant speed $v_x = 2.5 \ \mu m/s$ until a maximum displacement $x_{pip} = 90 \ \mu m$ (or strain $\delta/d = 0.6$) is achieved. The indenter is then held fixed for 4 s to eliminate any inertial effects before entering the unloading stage, where the indenter is moved upwards at the same speed $(-v_x)$ until it returned to its original position $(x_{pip} = 0)$.

Fig. 2b&c, shows examples of force-displacement responses of three different oocytes for the stress relaxation and loading-unloading experiment, as shown by the three color coded symbols, respectively. These two tests indicate the dual character of oocytes: on the one hand, they are able to elastically deform and store mechanical energy, as indicated by the presence of a remnant elastic force at the end of the relaxation test. On the other hand, they show a clear viscous response for which internal stresses decreases over time and dissipate mechanical energy, as indicated by the relaxation of stress and the hysteresis loops during the loading-unloading cycle. Furthermore, note that despite being all MII stage oocytes, there is a clear difference in the mechanical response which we attribute to the normal variability in biological systems.

B. Computational modeling of oocytes

Computational models are powerful assets to explore the detailed roles of material behavior on the deformation sustained by complex structures such as the oocyte. Ideally, a compelling model of the oocyte mechanics would account for the mechanics of the zona, the cytoplasm
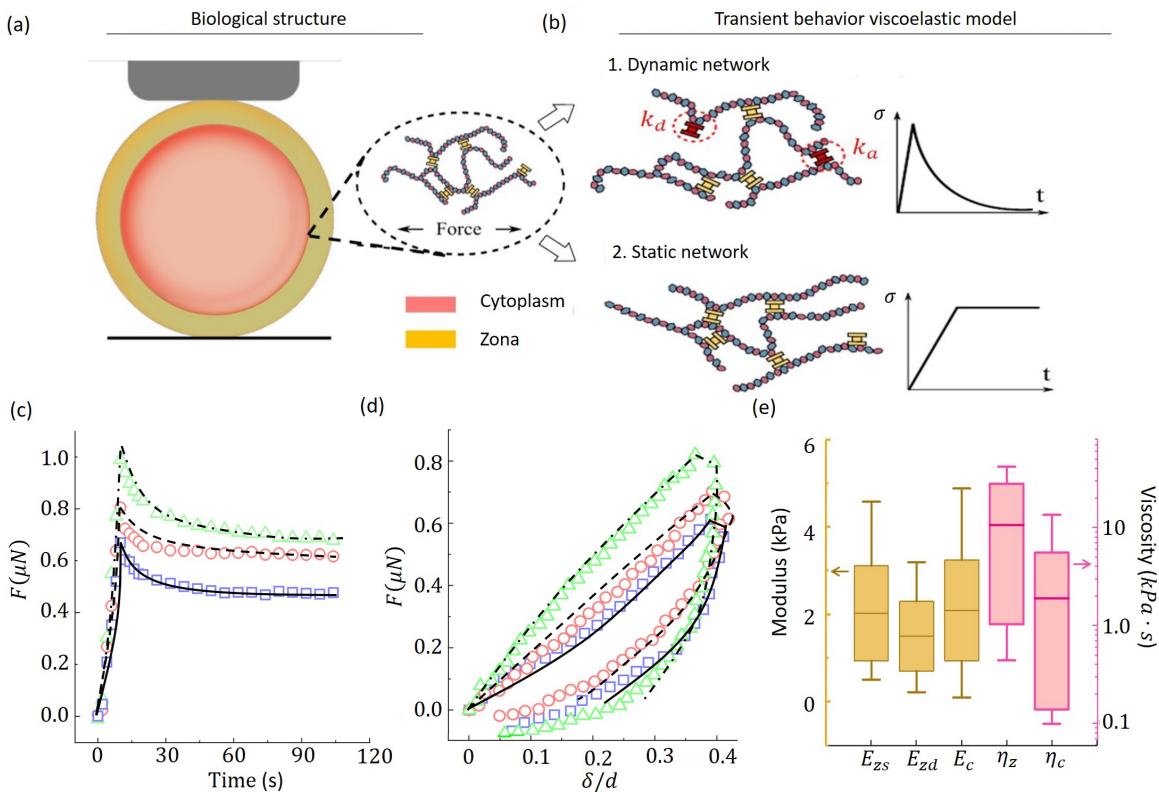
FIG. 3. *(a) Physical model of an oocyte body. (b) Conceptual understanding of a dynamic and static networks, and their response in stress relaxation test, respectively. Model fitting (black dashed lines) on the (c) stress relaxation, and (d) loading-unloading tests on the same three oocytes previously reported, represented by different symbols (gree triangle, red circle and blue square). (e) Summary on the range distribution of each fitted parameter.*

and the polar globe. However, to the best of our knowledge, the mechanical properties of the polar globe, and its directional effect on oocyte indentation are still unknown. Due to this missing information, as a secondary alternative, we here approximate the oocyte as a layered spherical body (Fig. 3a) composed only the cytoplasm and the zona, both of which are characterized by their own properties and distinct mechanical behavior. We then use the finite element method [52] to predict the oocyte deformation under various indentation loads and material parameters. These simulation results may then be identified with the corresponding experimental data to determine the properties of cytoplasm and zona pellucida of each oocyte tested experimentally. Biologically relevant events usually occur at the molecular scale, in which small modifications may modify the nature of the different biopolymer networks conforming the oocyte. Therefore, the way by which these networks mediate their elastic, time-dependent properties holds the key to understanding the relationship between biology and mechanics.

The zona and the cytoplasm are formed by a complex network of glycoproteins and cytoplasmic filaments, respectively [42, 53] which, from a modeling viewpoint,

can be classified as either static or dynamic depending on the nature in the cross-links and their mechanical response. Static networks are connected by permanent or very strong physical cross-links that can sustain the mechanical load, yielding a primary elastic response. Dynamic networks, on the other hand, are formed by weak physical cross-links that can constantly break and reform under the action of thermal fluctuations [49]. Recent theoretical models based on statistical mechanics [49, 54] have established a link between the visco-elastic response of the network and the cross-link density ρ, the entropic elasticity of single chains as well as their rate of detachment/reattachment (referred to as k_a and k_d, respectively). Macroscopically, dynamic networks exhibit a behavior that is close to a Maxwell-type elastic fluid with viscosity $\eta = E/k_d$ and instantaneous Young's modulus $E = 3\rho k_B T$ [49] while static networks only possess an elastic component (Fig.3b). As a result, a structure containing these two networks is able to simultaneously store elastic energy (as elastic solids) and dissipate energy (as viscous fluids) by stress relaxation from reconfiguring their topology.

In this context, the zona pellucida has been shown to be made of a network of at least three main glycopro-
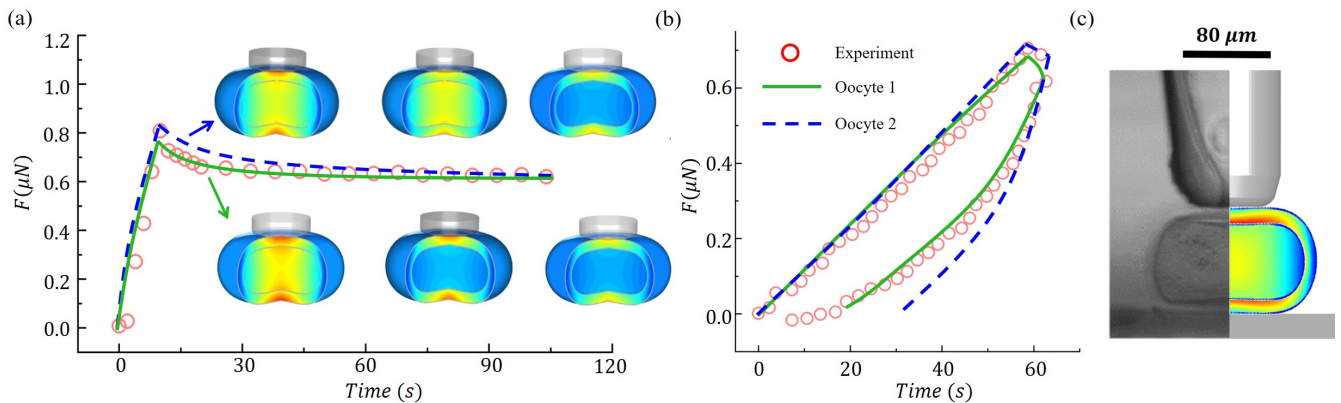
FIG. 4. *Example of a non-unique fitting solution where two oocytes with different properties show a similar response in (a) stress-relaxation and (b) loading-unloading tests. (c) A comparison about the deformation profile between finite element and experiment for oocyte 1.*

teins organized in bundles [53, 55–57]. Although it is widely accepted [58] that these filaments are cross-linked by non-covalent bonds, its mechanical behavior has been classically modeled as an incompressible elastic structure characterized by an elastic modulus E_z [59, 60]. The value of this modulus has has been estimated to range from $3kPa$ [48] to $17.9kPa$ [45] in mammalian oocytes (Fig. Ib) depending on the maturation stage [61–63]. However, this understanding of the zona has been challenged by the recent work of Papi et al. [64–66], who reported a substantial viscous response, the extent of which still has to be put into perspective. This current knowledge, together with our experimental results suggest that the zona contains both elastic and viscous components in its mechanical response and therefore may be described by the combination of an incompressible static network (with Young's modulus E_{zs}) and dynamic network (with Young's modulus E_{zd} and viscosity η_z). This is akin to synthetic polymers such as hydrogels with metal-ligand cross-links synthesized and engineered to contain these two types of networks to obtain similar mechanical properties.[67] Our understanding of the cytoplasm remains even more elusive. Our current knowledge mainly relies on studies performed on other types of cells, that can be of human origin [31, 34] or not [68]. In general, the cytoplasm is highly heterogeneous and made of clusters of densely packed and/or strongly cross-linked filaments separated by very soft or sol-like regions [42]. As a result, while there is a consensus that it primarily behaves as a viscous, non-Newtonian fluid, there are controversies regarding its viscosity, with reported values spanning several orders of magnitudes (Fig. Ic). This disparity may originate from the measurement method, where global experiments (over the entire cell) report viscosities around five to six orders of magnitude above water and microscopic rheology tests indicating viscosities closer to that of water [35]. Furthermore, a detailed modeling of the cytoplasm is hindered by the high heterogeneity arising from the presence of nucleus, organelles, and others. Due to this generalized uncertainty and based on its global mechanical behavior, we approximated the cytoplasm as a homogeneous medium modeled as a dynamic network (or elastic fluid) with instantaneous modulus E_c and viscosity η_c. To combine zona and cytoplasm into a single unit, we introduced a no-slip condition at the interface due to the viscous nature of both compartments. Finally, the contact between the indenter and the zona is approximated to be frictionless and mimicked by an artificial repulsive force (see supplemental information S1 for details) preventing the penetration of the two bodies. The coupled zona-cytoplasm model is implemented into a custom axisymmetric finite element framework to reproduce experimental conditions in silico. For more details on simulations, the reader is referred to previous work in [52, 69, 70].

We have thus identified a set of five parameters that can represent the complex visco-elastic response of the oocyte under various conditions: E_{zs}, E_{zd}, E_c, η_z and η_c. In other words, if an oocyte's malfunction is linked to its mechanical behavior, one may expect a correlation between these parameters and its chance of fertilization. However, as we will see below, the determination of these parameters from experiments is not trivial. Further discussion will therefore concentrate on this key challenge and its solution by the proposal of a standard protocol for oocyte characterization.

C. Oocyte characterization

To illustrate the potential challenges in characterizing and oocyte, let us consider the experimental data presented in Fig. Ic and attempt to determine the five material parameters using curve fitting. For this, we employ an inverse finite-element method (iFEM) that couples the standard finite-element model introduced above with an optimization algorithm, similar to the approach taken in [71]. Using this method, we are able to iden-

tify the parameters of oocyte properties that best fit the experimental data (details are shown in supplementary information). Previous studies [71, 72] have shown that one strategy to uniquely determine the oocyte mechanical properties consists in matching two main aspects: the force-displacement relation, and the deformed profile of the oocyte. In this study, however, this strategy was hindered by the transparency of the zona (Fig.1 a&b). Alternatively, to ensure the fitting accuracy, we obtained the material properties by simultaneously fitting stress-relaxation and loading-unloading tests for each different oocyte (Fig. 3c-d). In Fig.3e, we summarize the distribution of oocyte parameters that lead to a satisfactory match between the model and the experiments. We note that, while the moduli E_{zs}, E_{zd}, and E_c are both at the scale of $\sim kPa$, which corresponds to the range reported in the literature (Fig.Ic), the viscosity η_z and η_c span two orders of magnitude. This variability stems from the existence of a non-unique solution in fitting the experimental results, and which we attribute to the inability on separating the time-dependent properties of the cytoplasm and the zona solely from the overall response of the oocyte. To illustrate this point, let us consider two oocytes with different viscoelastic properties, but that exhibit a similar macroscopic response. The first oocyte is endowed with quickly relaxing zona ($\tau_z = \eta_z/(E_{zs} + E_{zd}) \sim 5s$) and a slowly relaxing cytoplasm ($\tau_c = \eta_c/E_c \sim 20 \ s$) while the second exhibits opposite properties, with $\tau_z \sim 20 \ s$ and $\tau_c \sim 5 \ s$, respectively. The respective macroscopic responses of these hypothetical cells presented in Fig. 4a-b illustrate that two choices of parameters can result in very similar stress relaxation and hysteresis responses. A closer investigation of the stored elastic energy in the oocyte (Fig.4a) confirms that the macroscopic response is due to different internal mechanisms; in the first oocyte, the elastic energy in the zona decreases to a constant value in less than 10 s (snapshot 1 to 2) while there is no obvious change in the cytoplasm due to its slow relaxation rate. At $t = 100 \ s$, the cytoplasm has finally relaxed, and the remaining force carrying capacity is due to the permanent network in the zona (snapshot 3). These effects are reversed in the second case, where the cytoplasm relaxes before the zona. Both of these two parameter sets satisfy the fitting criterion of the optimization scheme between the experimental and modeling results and their correctness can neither be judged according the existing literature, due to the great disparity in the reported values shown in Fig.1c, nor by their deformation profile, shown in the subfigures in Fig.4a, which also match the experimental measured profile, as shown by the example in Fig. 4c for the first oocyte. In this regard, previous studies have physically removed the zona from the oocyte body and separately measured its mechanical properties [28, 47]. However, these tests inevitably damage the oocytes and may induce changes in the properties of the zona. A new paradigm is, therefore, needed to measure the response of distinct oocyte compartments accurately.

III. DISTINCT ROLES OF ZONA AND CYTOPLASM: REDUCED MODEL AND IMPLICATIONS

Such heterogeneous mechanical response is indeed ubiquitous in biological materials such as bones [73], soft tissue [74, 75] and cells [76], where the roles of each constituent in the overall mechanical response vary with each type of loading. Thus, based on the insight given by the stored elastic energy in the previous section, we speculate that the involvement of the zona and the cytoplasm in the overall response can be controlled by varying the loading conditions (i.e., the width of the indenter and the indentation depth). For this, we present a solution based in two steps. We first derive a reduced model based on the force (F)-displacement (δ) relationship for indentations that cause small deformations in the oocyte. The parameters of this model are the five mechanical properties of the oocyte identified in Section II.B, which makes it more comprehensive and easier to analyze. Second, we discuss the limitations of this reduced model in correctly assessing the properties of the oocyte. Although this reduced model does not directly solve the problem of separating the roles of the zona and the cytoplasm, it led to an oocyte testing protocol that allows differentiating the contribution of each oocyte compartment.

A. A reduced model of oocyte indentation at small deformation

The reduced model is developed on the basis of Hertz's contact theory between two homogeneous elastic spheres, which is generalized based on Ting's solution [51] to account for the viscoelastic nature of the oocyte. Let us start by considering an oocyte of radius R_0 compressed by a rigid indenter whose bottom surface is approximated by a half-sphere of radius w. When the loading is displacement controlled (given $\delta(t)$), the force response of the oocyte is time dependent due to its viscoelasticity. In the regime of small deformation, the force (F)-displacement (δ) relationship can be described by a viscoelastic Boltzmann integral equation [77] and a time-dependent relaxation modulus $E_r(t)$ as follows:

$$F(t) = \frac{16}{9}\sqrt{R} \int_0^t \frac{d(\delta^{\frac{3}{2}})}{dt'} E_r(t-t')dt' \qquad (1)$$

where t' is the integration variable for time, and R is the effective contact radius defined by $1/R = 1/w + 1/R_0$. We note that the determination of the relaxation function $E_r(t)$ is based on two considerations. First, the oocyte is a heterogeneous body with two main compartments: the zona and the cytoplasm. Second, two dynamic networks
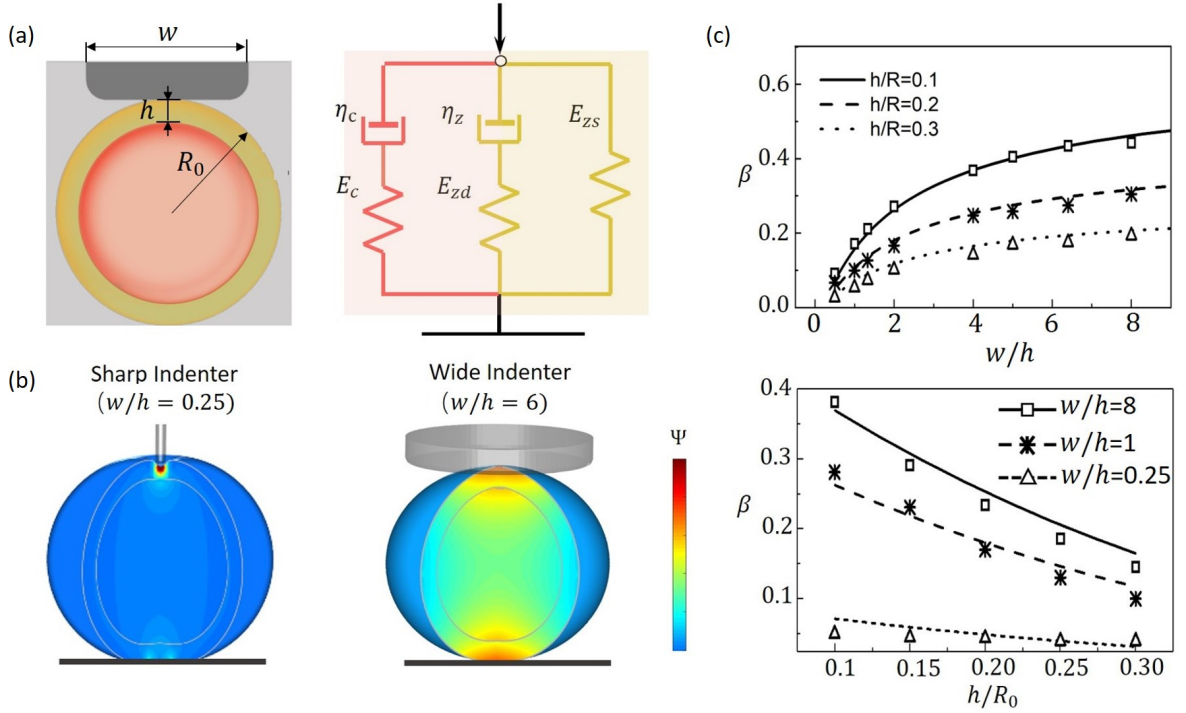
FIG. 5. *(a) Schematic illustration of oocyte structure and the generalized Wiechert model used to describe its viscoelastic behavior. (b) Finite element simulation showing the indentation by a sharp and wide indenter. The table shows the computation of effective modulus E and the relaxation modulus $E_r(t)$. (c) Calibration of β as a function of indenter width, measured by w/h, and zona thickness, measured by h/R_0.*

coexist in the oocyte, each of which contains an independent viscoelastic kinetic constant. To account for these two points, we introduce a weighted generalized Wiechert model [78], as shown in Fig. 5a, to describe the viscoelasticity of the oocyte. This model contains a parallel arrangement of two Maxwell elements, corresponding to the dynamic networks in the cytoplasm and the zona, respectively, and an elastic spring for the permanent network in the zona. To further specify the roles of each compartment in the overall response, we introduce a weight parameter $\beta \in [0, 1]$ that measures the fractional contribution of the cytoplasm and, hence, $1 - \beta$ describes the contribution of the zona. For this combination of parallel Maxwell elements, the relaxation modulus $E_r(t)$ takes the form:

$$E_r(t) = (1 - \beta)\left(E_{zs} + E_{zd}\, e^{-t/\tau_z}\right) + \beta E_c e^{-t/\tau_c} \quad (2)$$

where E_{zp} and E_{zd} are the Young's moduli of the permanent and dynamic networks of the zona, E_c is the Young's modulus of the cytoplasm, while τ_z and τ_c correspond to their respective relaxation times.

Experimental observations suggest that the above material parameters do not only depend on the thickness of the zona, measured by h/R_0, but are also sensitive to the relative size of the indenter w.r.t the zona, given by the ratio w/h [24, 71, 79]. In order to determine the dependence of β on these two parameters, let us consider

some extreme scenarios. First, when the zona is very thin, it acts like a membrane with negligible contribution to the overall response. On the other extreme, when the zona is very thick ($h/R_0 \to 1$), the oocyte becomes a monolayered sphere whose mechanical response is solely contributed by the zona. Regarding the effect of the indenter, when its width is small comparing to the zona thickness (small w/h), the deformation may be localized around the indenter and restricted to the zona. This results in the fractional contribution of the cytoplasm, β, to approach 0. (see Fig. 5b). As the indenter becomes wider, the deformation becomes more global and the cytoplasm is also involved in the mechanical response. Based on the above considerations, we approximated the effect of the zona thickness and the indenter width in a small deformation regime by the following form:

$$\beta = \left(1 - \frac{h}{R_0}\right)^m exp\left[-\left(\frac{w}{h}\right)^n\right]. \quad (3)$$

where m and n describe the sensitivity of β on h/R_0 and w/h, respectively. To quantify the value of these two parameters, we performed simulations of small rapid deformations ($\delta = 0.5\ h$) followed by stress relaxation for oocytes with different zona thickness ($h/R_0 \in [0.1,\ 0.2,\ 0.3]$ according to literature) and indenter widths ($w/h \in [0.25,\ 1,\ 8]$) (Fig. 5c). During the loading stage, the deformation was applied instantaneously such

that the loading time t_0 was much smaller than the relaxation time of the dynamic networks ($t_0 << \tau_z$ and $t_0 << \tau_c$). In this case, eq. 1 degenerates to a force-indentation relation given by $F = (16/9)\sqrt{R}\delta^{\frac{3}{2}}E_r(t_0 \rightarrow 0)$ in the loading stage, and $F(t) = (16/9)\sqrt{R}\delta^{\frac{3}{2}}E_r(t - t_0)$ in the relaxing state [80]. Using the above $F - \delta$ relationship, the relaxation modulus $E_r(t)$ was obtained for each set of zona and indenter sizes from finite element simulations. Using eq. 2, the value of the cytoplasm contribution parameter β was then fitted to simulation results (see Fig. 5c) and determined $m = 3$ and $n = -0.9$. The accuracy of the fit can be evaluated by the coefficient of determination, or the so-called r-squared number, that measures the fraction of variations between the finite element results that is described by the fitting function. In this case, the r-squared is 0.962, indicating an accurate fit between eq.(3) and the finite element results. Thus, as the zona becomes thicker (large h/R_0) its role becomes more pronounced and β decreases. Similarly, β decreases as the indenter becomes sharper (low w/h) where the deformation is mostly restricted to the zona as illustrated in Fig. 5. The force $F(t)$, in general, depends on both the relaxation modulus $E_r(t)$ and the loading history $\delta(t)$. For these more complex situations, the $F - \delta$ relationship of a mechanical experiment can be obtained by solving eq.1-2 by numerical approaches, such as the finite difference method [81]. This reduced model provides a critical tool to identify adequate experimental protocols for separating the distinct roles of zona and the cytoplasm.

B. Validity and limitations of the modified Hertz model.

As the reduced model is derived from a modified Hertz model, by definition it is invalid for large deformations due to the nonlinear change in contact area and the force-displacement relationship. Therefore, it is useful to determine the range accuracy of the proposed model to know its ability to accurately describe experimental measurements. Experimentally, the loading condition for oocyte indentation is controlled by three main parameters: the indenter width, the maximum indentation depth, and the loading rate. Since the effect of the indenter width has been analyzed in the previous section and characterized by eq. 3, we focus here on the effects of the indentation depth (normalized to the zona thickness, $\delta^* = \delta/h$) and the loading rate (relative to the zona relaxation time, $\zeta = \dot{\delta}\tau_z/h$). For this, we perform finite element simulations of oocyte indentation at constant rates to obtain its force-deformation behavior which is also separately calculated from the reduced model. The oocyte is endowed with material properties taken from the average values used to fit experiments shown in Fig. 3e while the indenter is given a width, $w = h$. Fig.6a compares the high fidelity finite element and the reduced model predictions of the $F - \delta$ relationship during the indentation at three different rates. As expected, the responses are

in good agreement at small indentation depths ($\delta^* < 1$), but the reduced model over-predicts the responsive force as the indentation increases ($\delta^* > 2$). This is because the deformation of the zona includes significant bending at large values of δ^*, which increasingly violates the compression assumption of the Hertz model and leads to an over-prediction of the response. The plot also indicates that the relative error in predictions from the reduced model rises quickly with deformation δ^* at slow loading compared to fast loading. To further quantify how the loading rate affects the validity of the model, the *in-silico* indentation test was performed for a wider range of loading rates ($\zeta \in [0.05, 10]$) and plotted in Fig. 6b as a relative error map for various loading rates and indentation depths. We see here that the error propagation in the model is significantly larger at smaller indentation depths for slow loading compared to fast loading. This
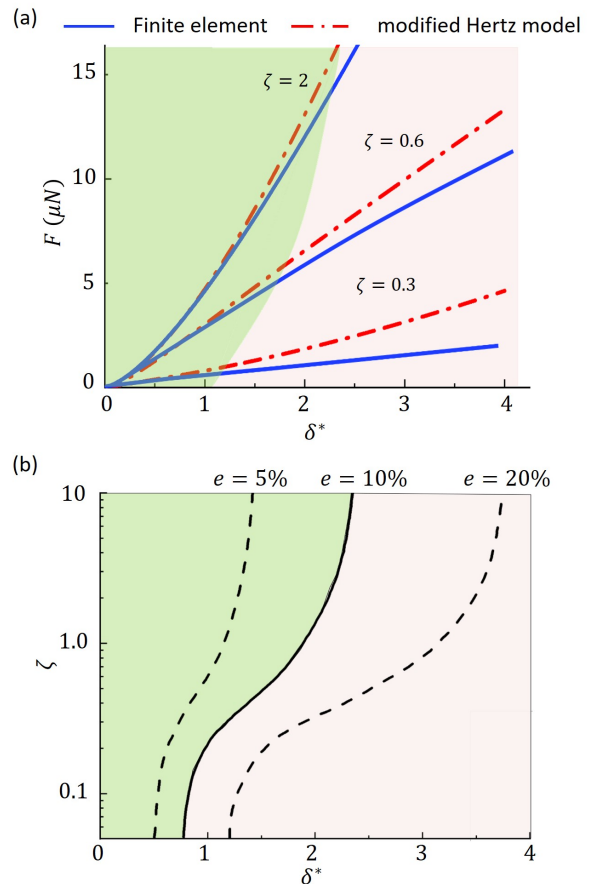
FIG. 6. *(a) Comparisons of the Finite Element analysis and the reduced model for the force-displacement curves at different loading rates $\zeta = \dot{\delta}^*\tau_z$, where τ_z is the relaxation time of the zona, δ is the displacement or indentation depth normalized to the zona thickness h. (b) Phase diagrams about the range of loading conditions at which the reduced model provides accurate predictions ($e < 10\%$) about the oocyte response. The dash lines depict the relative error of $e = 5\%$ and $e = 20\%$ made by the reduced model.*
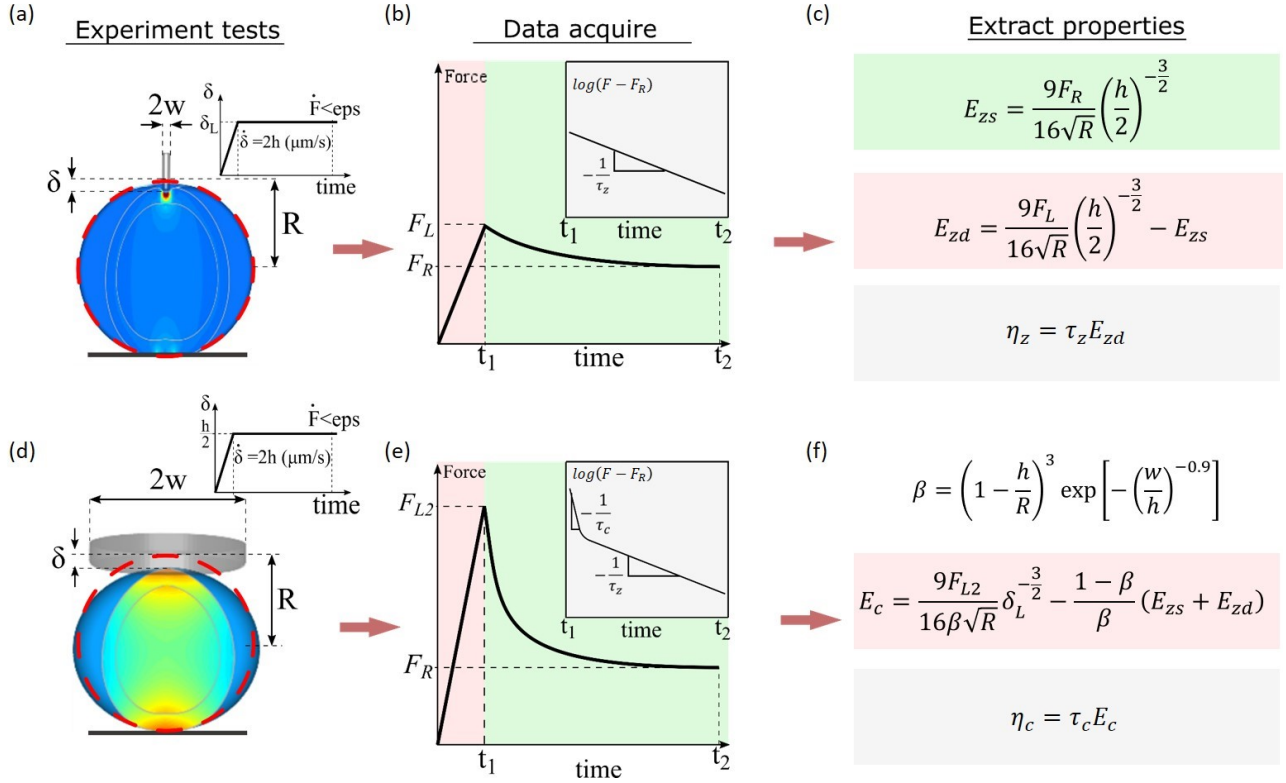
FIG. 7. *A protocol that can measure the properties of zona and cytoplasm with two consecutive tests. This protocol provides the instruction for (a)-(c) extracting the properties of zona via indentation relaxation test using a sharp indenter and (d)-(f) obtaining cytoplasm properties with a wide indenter.*

may be explained by the following reasoning; for slow loading, there is enough time for the cytoplasm to relax its stress causing the zona to take most of the load. This induces bending in the zona at small indentations ($\delta^* \approx 0.8$ for 10% error) making the reduced model inaccurate. For faster loading, both the zona and the cytoplasm are mechanically active in resisting the deformation without significant bending, and therefore allow for a larger indentation depth ($\delta^* \approx 2$ for 10% error) before the reduced model becomes significantly inaccurate.

C. A non-invasive and well-posed testing protocol.

To make the reduced model usable, knowing the range of its validity, we seek to identify an experimental protocol that yields a well-posed inverse problem. According to eq. 2, the role of the zona and the cytoplasm can be separated by controlling the weight parameter β via the indenter's size. In particular, one observes from eq. 3 that if the indenter size is relatively small ($w \ll h$), β converges to 0 and the measured moduli are those of the zona. In other words, a stress relaxation test with a sharp indenter is enough to determine the three parameters E_{zs}, E_{zd} and τ_z as shown in Fig. 7a-c. To determine the properties of the cytoplasm in a similar fashion, one may imagine experimental conditions for which β con-

verges to 1. However, Eq. 3 implies that this is not possible unless the zona is removed ($h = 0$). Instead, if one considers a large indenter size ($w \gg h$), eq. 3 shows that β converges to the value $(1 - h/R_0)^3$. In this case, we see from eq. 2 that both zona and cytoplasm are involved in the mechanical response of the oocyte. We show in Fig. 7d-f that the use of another simple stress-relaxation test with a large indenter is enough to determine the two remaining parameters E_c and τ_c.

Since two consecutive indentation tests are needed to fully determine the properties of the oocyte, it is critical that its viability is retained. For this, previous experiments on indentation [22] and micropipette aspiration [23] have shown that a deformation within 20% of the diameter can be considered to be non-invasive and would not lead to developmental malfunctions of the cell. Based on these considerations, we therefore propose a simple, non-invasive testing protocol that can be used to uniquely determine the distinct properties of the zona pellicuda and the cytoplasm in the oocyte. This protocol is depicted in Fig. 7 and can be summarized as follows:

1. The oocyte is subjected to a stress relaxation test conducted by a sharp indenter so that only the zona is deformed. As shown in the subfigure of Fig.7a, the compression is applied at a fast rate ($t_1 < 0.5s$) with a small indentation depth ($\delta \approx h/2$ or equiv-

alently $\delta \approx d/20$) so that the oocyte maintains its viability and the reduced model is accurate.

2. From the measured force-time relationship (Fig.7b), one can extract the properties of the zona E_{zs}, E_{zd} and τ_z using the analytical expressions given in Fig.7c.

3. The oocyte is subjected to the second experiment shown in Fig.7d, where the same indentation test is applied using a wider indenter so that the cytoplasm is also deformed. In this case, one should observe two different relaxation characteristic times in the measured force-time relationship (Fig.7e).

4. Based on the knowledge of zona properties, the properties of the cytoplasm can be readily calculated using the equations given in Fig.7f.

To verify whether this protocol provides an accurate extraction of oocyte properties, we performed *in silico* experiments using the finite element simulations, and evaluated the relative error made by the protocol in measuring the properties. The result is shown in the supplemental information (Fig. S3), where we see the protocol is able to extract the properties of 20 different oocytes of accuracy within 10% relative error. We note that, while the protocol shown in Fig.7 imposes a indentation depth of $\delta = h/2$, this value could be subject to variations depending on the experimental conditions with a resulting accuracy as depicted on Fig.6. We note, however, that both the error in the results, and the probability in damaging the oocyte are increased with the indentation depth.

IV. CONCLUSION

In summary, this paper presented a viscoelastic extension of the Hertz model to describe the mechanical behavior of oocytes under indentation. Particularly, the model incorporates the heterogeneity in the oocyte structure by assuming that the mechanical response is mostly dependent on two components: a thick outer layer made of biopolymers called zona pellucida and the cytoplasm. The model was validated with high-fidelity finite element simulations and calibrated with experiments on human oocytes. Despite its simplicity, this novel approach was able to accurately predict the viscoelastic response of oocytes as a function of (i) geometrical parameters such as cell radius and zona thickness, and (ii) loading conditions such as indentation rate, depth, and indenter size. Interestingly, we found that the mechanical deformation

of the zona pellucida and the cytoplasm can be decoupled by simply altering the size of the indenter. Thus, in addition to improving accuracy, the model has the potential to help develop new experimental protocols and improve the mechanical characterization of oocytes. Capitalizing on this, we finally proposed a non-invasive experimental protocol to uniquely characterize the viscoelastic properties of both major components of the oocyte. We note that although the introduction of the reduced model does not directly solve the issue of multiple solution in the literature. It simplifies the problem and provides a clear indication on how the roles of the cytoplasm and the zona can be controlled by varying the loading condition. This key finding finally leads to the development of the experimental protocol that can accurately measure the properties of each oocyte compartment. Besides, instead of having to implement the complicated inverse finite element method, researchers can readily apply the simple formula provided by the reduced model to extract the oocyte properties, which makes the protocol accessible to very broader communities.

The findings in this paper stress the relevance of computational models in the study of biological systems and bioengineering [82–84], where they not only help decrypt the underlying physics but also help in improving experimental strategies. As a start, this study assumed that both the zona and the cytoplasm are homogeneous bodies and their time-dependent response are only caused by the rearrangements of biopolymer networks. The effects of poroelasticity, solvent transport [85, 86], and adhesion [87] in the mechanical response are still poorly understood and are candidates to modify future models. Hence, we expect these results to motivate further experiments that would help to better understand the mechanics and dynamics of the oocyte and eventually tackle important questions such as the mechanical differentiation during zona maturation and fertilization[28, 66]. We also expect further development in experimental characterization technique that provides a clear profile of each compartment of the oocyte, which would increase the accuracy of modeling the oocyte mechanics through the inverse finite element method. Lastly, the reduced model and the protocol is only valid for small deformation and may loose their accuracy in the case of large deformation. Further studies will also generalize the reduced model so that it is useful for a wider range of loadings that involve large deformations and different indenter geometries.

[1] P. W. Farin, J. H. Britt, D. W. Shaw, and B. D. Slenning, Theriogenology **44**, 339 (1995).

[2] I. Boiso, A. Veiga, and R. G. Edwards, Reproductive biomedicine online **5**, 328 (2002).

[3] N. R. Mtango, S. Potireddy, and K. E. Latham, International Review of Cell and Molecular Biology **268**, 223

(2008).

[4] M. Stitzel and G. Seydoux, Science **316**, 407 (2007).

[5] L. Rienzi, B. Balaban, T. Ebner, and J. Mandelbaum, Human Reproduction **27**, 2 (2012).

[6] S. Bianchi, G. Macchiarelli, G. Micara, A. Linari, C. Boninsegna, C. Aragona, G. Rossi, S. Cecconi, and S. A. Nottola, Journal of Assisted Reproduction and Genetics **32**, 1343 (2015).

[7] S. Kahraman, K. Yakın, E. Dönmez, H. Şamlı, M. Bahce, G. Cengiz, S. Sertyel, M. Şamlı, and N. İmirzalıoğlu, Human Reproduction **15**, 2390 (2000).

[8] P. Xia, Human Reproduction **12**, 1750 (1997).

[9] T. Ebner, M. Moser, M. Sommergruber, M. Puchner, R. Wiesinger, and G. Tews, Human Reproduction **18**, 1294 (2003).

[10] J. S. Meriano, J. Alexis, S. Visram-Zaver, M. Cruz, and R. F. Casper, Human reproduction (Oxford, England) **16**, 2118 (2001).

[11] B. Balaban and B. Urman, Reproductive BioMedicine Online **12**, 608 (2006).

[12] G. Y. Lee and C. T. Lim, Trends in Biotechnology **25**, 111 (2007).

[13] C. A. Simmons, Journal of the American College of Cardiology **53**, 1456 (2009).

[14] S. Suresh, J. Spatz, J. P. Mills, A. Micoulet, M. Dao, C. T. Lim, M. Beil, and T. Seufferlein, Acta Biomaterialia **23**, S3 (2015).

[15] A. J. Engler, S. Sen, H. L. Sweeney, and D. E. Discher, Cell **126**, 677 (2006).

[16] W. Xu, R. Mezencev, B. Kim, L. Wang, J. McDonald, and T. Sulchek, PLoS ONE **7** (2012), 10.1371/journal.pone.0046609.

[17] G. D. Palermo, M. Alikani, M. Bertoli, L. T. Colombero, F. Moy, J. Cohen, and Z. Rosenwaks, Human reproduction **11**, 172 (1996).

[18] Y. Hiramoto, Experimental Cell Research **56**, 201 (1969).

[19] I. Nemoto, IEEE Transactions on Biomedical Engineering **BME-29**, 745 (1982).

[20] J. Abadie, C. Roux, E. Piat, C. Filiatre, and C. Amiot, Sensors and Actuators, B: Chemical **190**, 429 (2014).

[21] Y. Murayama, C. E. Constantinou, and S. Omata, Journal of Biomechanics **37**, 67 (2004).

[22] Y. Murayama, K. Yoshida, H. Takahashi, J. Mizuno, K. Akaishi, and H. Inui, Conference proceedings : ... Annual International Conference of the IEEE Engineering in Medicine and Biology Society. IEEE Engineering in Medicine and Biology Society. Annual Conference **2013**, 6834 (2013).

[23] L. Z. Yanez, J. Han, B. B. Behr, R. A. R. Pera, and D. B. Camarillo, Nature Communications **7**, 10809 (2016).

[24] M. Khalilian, M. R. Valojerdi, M. Navidbakhsh, M. Chizari, and P. Eftekhari-Yazdi, Advances in Bioscience and Biotechnology **04**, 679 (2013).

[25] X. Liu, R. Fernandes, A. Jurisicova, R. F. Casper, and Y. Sun, Lab on a chip **10**, 2154 (2010).

[26] X. Liu, J. Shi, Z. Zong, K. T. Wan, and Y. Sun, Annals of Biomedical Engineering **40**, 2122 (2012).

[27] L. Z. Yanez and D. B. Camarillo, Cerebral Cortex , 1 (2017), arXiv:1611.06654.

[28] M. Papi, R. Brunelli, L. Sylla, T. Parasassi, M. Monaci, G. Maulucci, M. Missori, G. Arcovito, F. Ursini, and M. De Spirito, European Biophysics Journal **39**, 987 (2010).

[29] K. L. Sung, G. W. Schmid-Schönbein, R. Skalak, G. B. Schuessler, S. Usami, and S. Chien, Biophysical Journal **39**, 101 (1982).

[30] A. M. Mastro, M. A. Babich, W. D. Taylor, and A. D. Keith, Proceedings of the National Academy of Sciences **81**, 3414 (1984).

[31] P. A. Valberg and D. F. Albertini, Journal of Cell Biology **101**, 130 (1985).

[32] P. A. Valberg and H. A. Feldman, Biophysical Journal **52**, 551 (1987).

[33] K. L. Sung, C. Dong, G. W. Schmid-Schönbein, S. Chien, and R. Skalak, Biophysical Journal **54**, 331 (1988).

[34] E. Evans and a. Yeung, Biophysical journal **56**, 151 (1989).

[35] K. Fushimi and A. S. Verkman, Journal of Cell Biology **112**, 719 (1991).

[36] W. Stahlhofen and W. Möller, Radiation and Environmental Biophysics **32**, 221 (1993).

[37] R. E. Waugh and M. A. Tsai, "Shear Rate-Dependence of Leukocyte Cytoplasmic Viscosity," in *Cell Mechanics and Cellular Engineering*, edited by V. C. Mow, R. Tran-Son-Tay, F. Guilak, and R. M. Hochmuth (Springer New York, New York, NY, 1994) pp. 33–44.

[38] M. Sato, N. Ohshima, and R. Nerem, Journal of Biomechanics **29**, 461 (1996).

[39] G. Ragsdale, J. Phelps, and K. Luby-Phelps, Biophysical Journal **73**, 2798 (1997).

[40] O. Thoumine and A. Ott, Journal of cell science **110 (Pt 1**, 2109 (1997).

[41] A. R. Bausch, F. Ziemann, A. A. Boulbitch, K. Jacobson, and E. Sackmann, Biophys. J. **75**, 2038 (1998).

[42] a. R. Bausch, W. Möller, and E. Sackmann, Biophysical journal **76**, 573 (1999), arXiv:NIHMS150003.

[43] B. R. Daniels, B. C. Masi, and D. Wirtz, Biophysical Journal **90**, 4712 (2006).

[44] C. Margraves, K. Kihm, S. Y. Yoon, C. K. Choi, S. H. Lee, J. Liggett, and S. J. Baek, Biotechnology and Bioengineering **108**, 2504 (2011).

[45] Y. Sun, K.-T. Wan, K. P. Roberts, J. C. Bischof, and B. J. Nelson, IEEE transactions on nanobioscience **2**, 279 (2003).

[46] Y. Murayama, M. Yoshida, J. Mizuno, H. Nakamura, Y. Watanabe, K. Akaishi, H. Inui, C. E. Constantinou, and S. Omata, Bio One **25**, 8 (2008).

[47] M. Papi, L. Sylla, T. Parasassi, R. Brunelli, M. Monaci, G. Maulucci, M. Missori, G. Arcovito, F. Ursini, and M. De Spirito, Applied Physics Letters **94**, 1 (2009).

[48] M. Khalilian, M. Navidbakhsh, M. R. Valojerdi, M. Chizari, and P. E. Yazdi, Journal of the Royal Society, Interface / the Royal Society **7**, 687 (2010).

[49] F. J. Vernerey, R. Long, and R. Brighenti, Journal of the Mechanics and Physics of Solids **107**, 1 (2017).

[50] R. Brighenti, R. Menzel, and F. J. Vernerey, Journal of the Mechanics and Physics of Solids (2018).

[51] T. C. T. Ting, Journal of Applied Mechanics **33**, 845 (1966).

[52] L. Foucard, A. Aryal, R. Duddu, and F. Vernerey, Computer Methods in Applied Mechanics and Engineering **283**, 280 (2015).

[53] P. M. Wassarman, C. Liu, and E. S. Litscher, Journal of cell science **109 (Pt 8**, 2001 (1996).

[54] T. S. S. L. S. Vernerey, Franck J. and R. J. Wagner, Journal of Royal Society Interface (2018).

[55] J. M. Greve and P. M. Wassarman, Journal of Molecular

Biology **181**, 253 (1985).

[56] D. P. Green, Reviews of reproduction **2**, 147 (1997).

[57] R. Ungerfeld, A. L. Dago, E. Rubianes, and M. Forsberg, Reproduction, nutrition, development **44**, 89 (2004).

[58] P. M. Wassarman, "Zona pellucida glycoproteins," (2008).

[59] A. Vinckier and G. Semenza, in *FEBS Letters*, Vol. 430 (1998) pp. 12–16.

[60] J. Domke, S. Dannöhl, W. J. Parak, O. Müller, W. K. Aicher, and M. Radmacher, Colloids and Surfaces B: Biointerfaces **19**, 367 (2000).

[61] Y. Murayama, J. Mizuno, H. Kamakura, Y. Fueta, H. Nakamura, K. Akaishi, K. Anzai, A. Watanabe, H. Inui, and S. Omata, Human cell **19**, 119 (2006).

[62] E. Z. Drobnis, J. B. Andrew, and D. F. Katz, Journal of Experimental Zoology **245**, 206 (1988).

[63] M. Khalilian, M. Navidbakhsh, M. Rezazadeh Valojerdi, M. Chizari, and P. Eftekhari Yazdi, Experimental Mechanics **51**, 175 (2011).

[64] M. Papi, A. Maiorana, C. Douet, G. Maulucci, T. Parasassi, R. Brunelli, G. Goudet, and M. De Spirito, Applied Physics Letters **102** (2013), 10.1063/1.4789503.

[65] A. Boccaccio, L. Lamberti, M. Papi, M. De Spirito, C. Douet, G. Goudet, and C. Pappalettere, Interface Focus **4**, 20130066 (2014).

[66] A. Boccaccio, M. C. Frassanito, L. Lamberti, R. Brunelli, G. Maulucci, M. Monaci, M. Papi, C. Pappalettere, T. Parasassi, L. Sylla, F. Ursini, and M. De Spirito, Journal of The Royal Society Interface **9**, 2871 (2012).

[67] S. C. Grindy, M. Lenz, and N. Holten-Andersen, Macromolecules **49**, 8306 (2016).

[68] F. Crick and A. Hughes, Exp. Cell Res. **1**, 37 (1950).

[69] L. Foucard and F. J. Vernerey, International Journal for Numerical Methods in Engineering **107**, 923 (2016), arXiv:1010.1724.

[70] T. Shen, R. Long, and F. Vernerey, Computational Mechanics , 1 (2018).

[71] J. Dittmann, A. Dietzel, and M. Boel, Journal of the mechanical behavior of biomedical materials **77**, 764 (2018).

[72] K. Liu, D. Williams, and B. Briscoe, Physical Review E **54**, 6673 (1996).

[73] J.-Y. Rho, L. Kuhn-Spearing, and P. Zioupos, Medical engineering & physics **20**, 92 (1998).

[74] T. Courtney, M. S. Sacks, J. Stankus, J. Guan, and W. R. Wagner, Biomaterials **27**, 3631 (2006).

[75] D. M. Ebenstein and L. A. Pruitt, Nano Today **1**, 26 (2006).

[76] Y. M. Efremov, A. X. Cartagena-Rivera, A. I. Athamneh, D. M. Suter, and A. Raman, Nature protocols , 1 (2018).

[77] K. L. Johnson, *Journal of the American Chemical Society*, Vol. 37 (1985) pp. 1–17.

[78] S. Moreno-Flores, R. Benitez, M. d.M. Vivanco, and J. L. Toca-Herrera, Journal of Biomechanics **43**, 349 (2010).

[79] A. Boccaccio, L. Lamberti, M. Papi, M. De Spirito, and C. Pappalettere, Nanotechnology **26** (2015), 10.1088/0957-4484/26/32/325701.

[80] D. Gutierrez-Lemini, *Engineering Viscoelasticity* (2014) pp. 1–353.

[81] E. Isaacson and H. B. Keller, *Mathematics of Computation*, Vol. 21 (1967) p. 517.

[82] U. Akalp, S. Chu, S. C. Skaalure, S. J. Bryant, A. Doostan, and F. J. Vernerey, Polymer (United Kingdom) **66**, 135 (2015), arXiv:15334406.

[83] U. Akalp, S. J. Bryant, and F. J. Vernerey, Soft Matter **12**, 7505 (2016).

[84] S. L. Sridhar, M. C. Schneider, S. Chu, G. De Roucy, S. J. Bryant, and F. J. Vernerey, Soft Matter **13**, 4801 (2017).

[85] F. J. Vernerey, International Journal of Solids and Structures **48**, 3129 (2011).

[86] F. J. Vernerey, Transport in Porous Media , 815 (2012).

[87] F. J. Vernerey and M. Farsad, Journal of Mathematical Biology **68**, 989 (2014), arXiv:NIHMS150003.